

Geological and Geophysical Evaluation of the Mechanisms of the great 1899 Yakutat Bay Earthquakes

George Plafker and Wayne Thatcher

U. S. Geological Survey, Menlo Park, CA 94025

Abstract. We have used tectonic, geologic and seismologic observations to reevaluate the mechanisms and seismotectonic significance of the two great M_w 8.1 and 8.2 September 1899 Yakutat Bay earthquakes. In their comprehensive study of these earthquakes between 1905 and 1910, *Tarr and Martin* [1912] showed these events were accompanied by shoreline changes in Yakutat Bay that ranged from 14.4 m emergence to 2.1 m submergence, uplift of about 1 m at Yakataga 160 km west of Yakutat Bay, and by several zones of surface fissures on land. Although major earthquake faults were not found, *Tarr and Martin* postulated that the shoreline displacements were caused by vertical movements on a system of concealed steep normal faults and that the fissure zones on ridges were along subsidiary faults. Our geologic studies in the Yakutat Bay region indicate that: (1) the emergent shorelines along Yakutat Bay define a broad upwarp roughly 50 km by 30 km that is primarily related to reverse slip on local concealed shallowly-dipping thrust faults; (2) the reported subsidence was due largely, or entirely, to non-tectonic surficial submergence of unconsolidated deposits; and (3) most, if not all, of the zones of surface fractures related to the 1899 earthquakes are "sackung" that were probably caused by large-scale gravitational slumping of steep slopes, rather than faulting. A small number of early damped seismograms and the vertical uplift data were used to constrain the fault slippage that occurred during the two great earthquakes of 1899. Seismic moments determined from 50-sec. surface wave amplitudes are $\sim 2 \times 10^{21}$ N-m for these two events, equivalent to M_w 8.1. Uplift determined from raised shorelines within Yakutat Bay can be accounted for by the 10 September event alone, and these data can be fit by ~ 10 – 20 m dip slippage on three dextral oblique thrust faults that dip $\sim 30^\circ$ northeast or north. Faulting complexity is also shown by the S-wave seismogram of the 10 September shock, which lasted ~ 3 minutes and shows at least three distinct long-period pulses. The large seismic moment of the 04 September event and uplift of ~ 1 m at Yakataga suggest a 150 km westward extension of faulting along the foothills fold and thrust zone. Our reassessment suggests that, although some portions of the complex plate boundary zone ruptured in 1899, regional seismic hazard is currently significant. First of all, none of the potentially tsunamigenic offshore thrust faults west of the Pamplona zone slipped in 1899. It is unlikely that all of the onshore thrust faults south of the Chugach-St Elias thrust fault system did either. Furthermore, more than 100 years of convergence at 48 mm/yr across the region has reloaded faults that slipped in 1899 and added further strains on those that did not. Matters are much less clear for the Yakutat Bay thrusts because although they slipped in 1899 we have no good constraints on the convergence rates across these faults. The most recent pre-1899 uplift event in Yakutat Bay was at least 380 ± 70 years ago.

1. Introduction

The 1899 Yakutat Bay earthquake sequence occurred within the Yakutat block, an allochthonous miniplate that is moving northwestward at 48 mm/yr relative to North America. The earthquakes were located in a structurally complex angular join between the northwest-trending Fairweather transform, the west-trending system of thrust faults and oblique thrust faults along the northern boundary of the Yakutat terrane, and the Pamplona zone of thrust faults that trend southwest obliquely across the Yakutat terrane to connect with the Aleutian megathrust (Figure 1).

The 1899 earthquakes provide the earliest known instance of uplift at a coast that was attributed to faulting rather than regional warping, and they also retain the record for the greatest known onshore vertical displacement in a single seismic event (14.4 m uplift). In this paper, we apply new understanding of the tectonic setting, surface deformation, and original seismograms to better constrain the 1899 sequence. This knowledge is essential to determine the extent to which these events have relieved strain along the southern Alaska continental margin and to better assess which segments of the plate margin have relatively high potential for a future major earthquake.

1.1 Geographic Setting

The 1899 earthquakes are located at the eastern end of the Saint Elias Mountains in Alaska and adjacent parts of the Yukon Territory between Yakutat Bay and Yakataga (Figure 1). This region is characterized by high, rugged, generally east-west trending mountain ranges that contain extensive icefields and glaciers and the second and fourth highest peaks on the North American continent (Mount Logan, 6051 m and Mount Saint Elias, 5490 m). Many other peaks and ridges in the vicinity rise above 4300 m. Much of the mountains are covered by ice fields and glaciers that flow southward into Icy Bay, Malaspina Glacier, and Yakutat Bay or westward into Bering Glacier. Outwash deposited by energetic braided glacial streams, glacial moraine, and beach deposits, comprise a lowland of variable width along much of the coast shown in Figure 1.

1.2. The Earthquake Sequence

The 1899 Yakutat Bay earthquakes involved a series of events that were widely felt during a period of 26 days extending from September 4th to 29th. Hundreds of shocks were felt locally, and 4 or 5 events were recorded worldwide. The most severe earthquakes appear to have been the initial Mw 8.1 shock on September 4th and shocks of ~Ms 7.4 and Mw8.2 on September 10th (Table 1). Seismograms were few, but are sufficient to place the epicenters of the September 4th and 10th events in the vicinity of Yakutat Bay and Icy Bay (Figure 1) [Doser, 2006] and have provided data from which Abe & Noguchi [1983] have estimated the surface wave magnitudes.

As reported by Tarr and Martin [1912], the earthquakes were strongly felt throughout the Gulf of Alaska region. However, they caused no loss of life and only minor damage to property at Yakutat (population less than 300 in 1900 census) and the other small coastal settlements of Katalla, Yakataga and Dry Bay (Figure 1) due to the sparseness of the population, and the fact that buildings in the meizoseismal area were mostly one-story wood cabins. The September 4th event was felt on the lower Yukon

River at distances up to 1170 km from Yakutat Bay. It involved minor uplift of the coast near the settlement of Yakataga and reportedly also caused widespread seiches, avalanches, and visible ground waves in southern Alaska. The larger September 10th event, which climaxed the sequence, occurred on a day during which more than 50 shocks were felt in the Yakutat Bay area, five of which were felt 300 km to the northeast on the Yukon River. The two largest shocks of the day were recorded on seismographs around the world. The earlier large shock of Ms7.4, at about 8:00 a.m. local time was felt at distances of up to 400 km. The main shock, at 12:22 p.m. local time, was everywhere reported as the greatest disturbance of the series. It was felt to distances of 700 km from Yakutat Bay—somewhat less than the event of September 4th. However, the ground motion generated seiche waves at Lake Chelan, Washington, more than 1900 km distant. In the Yakutat Bay area the main event involved large-scale vertical changes in shorelines relative to sea level. There were also avalanches, probable submarine sliding, a local tsunami in Yakutat Bay, calving of tidal glaciers, and widespread surficial effects in unconsolidated deposits throughout the Yakutat region.

1.3 Previous Investigations and Present Study

Field investigation of earthquake effects in the meizoseismal area was carried out by a U.S. Geological Survey field party led by Dr. Ralph S. Tarr and Lawrence Martin mainly in the summer of 1905, but with incidental observations by one or both of them in 1906, 1909, and 1910. They mapped in detail the coseismic changes and local tsunami damage along the shores of Yakutat Bay, Disenchantment Bay, Russell Fiord, and Nunatak Fiord (Figure 2). Their pioneering observations, together with compilation of relevant information from eyewitnesses and published accounts in this sparsely inhabited area, are the primary sources of data available on the tectonic effects of the 1899 sequence [*Tarr and Martin*, 1906, 1912; *Martin*, 1910]. Except as otherwise noted, our citations to Tarr and Martin's work will be to their comprehensive 1912 Geological Survey Professional Paper because it incorporates essentially all the data presented in earlier publications on the 1899 earthquakes.

Our work on the 1899 earthquakes includes a field study of the neotectonics of the Yakutat Bay and Yakataga coastal areas by Plafker and colleagues carried out intermittently between 1967 and 2000 together with an analysis of the seismograms and modeling of coastal uplift by Thatcher. The data were used to reinterpret the magnitudes of the larger earthquakes and the pattern of coseismic deformation, and to reconstruct a revised model for the earthquakes that is compatible with our understanding of the tectonics of the source region.

2. Geologic and Tectonic setting

The part of the Chugach and Saint Elias Mountains that includes the 1899 epicentral region lies within the allochthonous, fault-bounded Yakutat terrane which is characterized by Cenozoic sedimentary and volcanic rocks overlying basement rocks of variable lithology and age (Figure 1). Except as otherwise noted, the following summary of the geology of the Yakutat terrane and adjacent regions is from *Plafker et al* [1994a]. For detailed discussions of the tectonic evolution of the terrane and major structural

features shown on Figure 1, see *Plafker et al.*, [1994a], *Bruhn et al.*, [2004], and *Pavlis et al.*, [2005].

The western and central parts of the Yakutat terrane are bounded on the west by the Ragged Mountain-Kayak Island zone, on the north by the Chugach-Saint Elias fault system, on the south by the Transition fault system and on the east by the Dangerous River zone. It is characterized by a sequence of more than 12,000 m of Eocene and younger continental, paralic, and marine predominantly clastic sedimentary rocks that are locally intruded by mafic plugs and dikes. The bedded rocks are highly deformed in a fold and thrust belt between the Kayak Island zone and the Pamplona zone-Malaspina system of faults; they are only gently deformed to the east between these faults and the Dangerous River zone. These two segments of the Yakutat terrane are underlain by Eocene oceanic crust.

The wedge-shaped area that makes up the eastern part of the Yakutat terrane is roughly bounded on the northeast by the Fairweather fault, on the north by the Coal Glacier fault, on the south by the Transition fault, and on the west by the Dangerous River Zone. It consists of Tertiary sedimentary rocks that unconformably overlie, or are in fault contact with, a basement of highly deformed and variably metamorphosed Late Cretaceous flysch and melange into which are intruded mid-Cretaceous to mid-Tertiary felsic to gabbroic plutons and Tertiary mafic plugs and dikes.

The Yakutat terrane is in fault contact with tectonostratigraphic sequences on the north and northeast consisting of Mesozoic flysch and oceanic volcanic rocks intruded by Eocene plutons (Chugach Terrane), on the west by Paleocene and lower Eocene flysch and oceanic volcanic rocks intruded by Eocene to middle Tertiary plutonic rocks (Prince William terrane), and on the south by the Pacific plate consisting of Paleogene oceanic basalt overlain by undeformed Eocene and younger poorly consolidated sedimentary strata.

With respect to the North American plate, the Pacific plate is moving to the northwest at 48 mm/yr [*Demets et al.*, 1994], parallel to the Fairweather-Queen Charlotte dextral fault system. Analysis of GPS data suggests there is ~10–30 mm/yr of relative motion between the Pacific plate and Yakutat terrane across the Transition Fault, with the remainder of the Pacific-North America motion occurring across the zone of compressive folding and faulting in the northern and western part of the Yakutat terrane and extending northward into the Chugach Mountains [*Fletcher and Freymueller*, 1999].

In the part of the Yakutat terrane west and north of the Pamplona-Malaspina zone of faults, the Cenozoic sequence on land and extending offshore to the Pamplona zone and Aleutian Trench, is commonly folded into a series of tight, asymmetric anticlines with steep to overturned faulted south limbs and intervening broad synclines (Figure 1). This zone of deformation, referred to herein as the late Cenozoic fold and thrust belt, extends to the western and southern boundaries of the Yakutat terrane. It is basically an extension of the wide eastern Aleutian zone of compressive deformation that extends across the offshore and onshore Yakutat terrane to a complex trench-transform triple junction with the Fairweather fault system in the Yakutat Bay area. In contrast, coeval sedimentary rocks south and east of the Pamplona-Malaspina-Yakutat system of faults are on a part of the Yakutat terrane that is coupled relatively tightly to the Pacific plate so that the sedimentary sequence is largely unaffected by late Cenozoic deformation except locally along the margins.

Inferred surface faults along which vertical shoreline displacements occurred in the region affected by the 1899 earthquakes are shown on Figure 1 (red). Many of the other faults within the Yakutat terrane have had known or suspected late Cenozoic displacements [Plafker *et al.*, 1994b]. They include the Fairweather fault along which dextral coseismic displacements of at least 4 m, and possibly as much as 6m, occurred along its entire exposed onshore length of 225 km during the great M 7.9 Lituya Bay earthquake in 1958 [Miller, 1960; Tocher, 1960]. Long-term slip on the fault has offset several valley glaciers and drainages including the 6 km offset of the east and west arms of Nunatak Fiord [Plafker *et al.*, 1978]. To the northwest of the Yakutat Bay area the fault trace is concealed by valley glaciers and ice fields of the Saint Elias Mountains. It may extend into the system of west- to northwest-trending, north-dipping thrust or oblique thrust faults west of the head of Yakutat Bay and some of the slip may be partitioned onto a splay fault north of the main trace that extends across the ice fields into the Alaska Range. The northern boundary of the Yakutat terrane, the Chugach-Saint Elias fault system (CSFS), dips roughly 30° north where it is exposed on ridges along the south flank of Mt. Saint Elias. Thrust faults to the south generally dip north at angles of 30° to 60°. The Esker Creek fault is a concealed fault on the west side of Disenchantment Bay at the head of Yakutat Bay (Figure 1, inset) that juxtaposes Cretaceous flysch on the north against Eocene coal-bearing strata on the south. The Sullivan fault (SF) near Yakataga is a north-dipping thrust in Neogene strata on the overturned south limb of the Sullivan Anticline [Miller, 1957]. To the west; it extends southwestward offshore; its eastern extent is not known. A significant component of northeast-directed contractional deformation between the Fairweather fault and the coast between Dry Bay and the Lituya Bay area (Figure 1) is indicated by (1) a tight anticlinal fold in Pliocene and older marine strata that is overturned towards the southwest and (2) a series of late Holocene marine terraces that undoubtedly formed by coseismic uplift steps at a long term average uplift rate of ~10 mm/yr [Miller, 1961; Hudson *et al.*, 1976; Bruhn *et al.*, 2004].

3. 1899 Deformation

During the summer of 1905, *Tarr and Martin* [1912] mapped and measured vertical displacements relative to sea level of the shorelines along the coast of Yakutat Bay, Disenchantment Bay, Russell Fiord, and Nunatak Fiord over a minimum area of about 1500 square kilometers (Figure 2). The most pronounced effects were regional changes in shoreline elevation in the Yakutat area, mainly involving uplift of as much as 14.4 m. In some localities emergent shorelines alternated with regions of no change or as much as 2.1 m of local submergence.

Tarr and Martin [1912] found the usual textbook examples of shoreline uplift, including wave-cut benches, sea caves, and uplifted beaches with the decaying remains of intertidal organisms. At a few places, submergence was indicated by the presence of terrestrial brush or trees submerged below the high tide line. All the physiographic evidences of vertical shoreline changes were identical with those seen following the great 1964 Alaska earthquake in the coastal region that extends some 800 km west of the Bering Glacier [Plafker, 1969].

There can be little doubt that tectonic deformation in the Yakutat Bay area occurred at the time of the great earthquake of September 10th, because the shoreline

changes in the Yakutat Bay area were witnessed by eight prospectors who happened to be camped at the head of Yakutat Bay during the earthquake. The prospectors in Yakutat Bay also reported violent waves during the earthquakes that washed away most of their camp and supplies. These waves were probably caused in part by the large coseismic uplift of shorelines in Disenchantment Bay, but were also due to calving of the front of Hubbard Glacier, and submarine slide-generated waves along the larger delta fronts. The prospectors' harrowing experiences during the sequence of violent shocks and destructive water waves as well as their subsequent perilous journey back to Yakutat in two small makeshift boats are reported in considerable detail by *Tarr and Martin* [1906, 1912].

At Yakataga, 160 km west of Yakutat, uplift of the rock reef fronting the settlement was noted by residents almost immediately after the September 4th event as a lowering of tide levels by about one meter (3 feet). Unlike the Yakutat Bay area, there were no shoreline changes at Yakataga during the main shock of September 10th. Although the earthquakes were strongly felt at a small native settlement in Dry Bay, 90 km southwest of Yakutat, there were no reports of changes in shorelines associated with either of the main shocks.

3.1. Shoreline Displacements in the Yakutat Bay Area

Tarr and Martin [1912] inferred a complex system of faults associated with the September 10th earthquake. Their conclusions were based largely on differential vertical displacements of opposing shores along bays and fiords and along the southeastern shore of Yakutat Bay (Figure 2). These faults were considered to be mainly steep normal faults. In *Tarr and Martin's* [1912] interpretation, crustal blocks were displaced and tilted to account for the observed bewildering pattern of vertical shoreline changes, particularly those in which uplift and subsidence occurred along the shoreline in close proximity. None of the faults mapped by *Tarr and Martin* [1912] in the area have surface expressions indicative of young displacement. Such features, however, are difficult to locate in this area of rugged topography; locally thick brush and forest; extensive water, ice, and snow cover; and rapid fluvial sedimentation.

By contrast, much of the evidence for shoreline uplift noted by Tarr and Martin in 1905 is still discernible along the coast despite the growth of brush and forest on emergent surfaces (Figures 3 and 4; online Appendix A). Reexamination of most of the shoreline localities visited by *Tarr and Martin* [1912] was carried out intermittently by one of us (G.P.) during the course of geologic mapping in the region between 1967 and 2000 (online Appendix B). We then re-evaluated the vertical displacements reported by *Tarr and Martin* [1912] in the light of new geologic mapping in the Yakutat Bay area and studies of the effects of earthquake-related shoreline displacements elsewhere.

Our studies indicate that measured uplift values by Tarr and Martin are still generally reproducible. Two major exceptions, however, are a 10-km-long segment of Logan Beach on the eastern shore of Yakutat Bay and the shoreline at the south end of Russell Fiord (see Figure 2 for locations).

At Logan Beach, subsidence was reported along an inferred fault in an area of unconsolidated older Holocene glacial deposits and extensive destruction of shoreline forests by local tsunami waves up to 12 m high [*Tarr and Martin*, 1912, Plate 19A, 19B]. In this area, the inner margin of the uplifted marine terrace is still visible at several

localities where it is marked by a uniform age forest that postdates uplift of the terrace in 1899 (Figure 3). Timber growth monitoring survey locations on the 1899 terrace both north and south of Logan Beach by the U.S. Forest Service [V.J. Labau, Forestry Sciences laboratory, written comm., 11/01/1982] show that the average tree age of the sample population is only 3–4 years younger than the 1899 uplift and the oldest trees on the surface date to 1899. Trim-line elevations of 4+ m were measured in 1979 along segments of the Logan Beach coast where the 1905 data indicate either no change or subsidence (Figure 2).

At the south end of Russell Fiord, small bedrock outcrops are interspersed among extensive deposits of a terminal moraine that dams the south end of the fiord. Although the bedrock outcrops were uplifted 2 to 3 meters, some moraine deposits showed clear evidence of shoreline submergence where trees were tilted and slumped into the fiord. *Tarr and Martin* [1912] observed that several of these areas were still moving seaward in 1905. One large slide in till they described at the extreme south end of the fiord (see Figure 2 for location) was actively slumping into the fiord when visited in 1980, possibly as a result of reactivation during the 1958 Lituya Bay or other earthquakes. After the 1958 M7.9 Lituya Bay earthquake on the Fairweather fault, extensive areas of surficial compaction, slumping, and liquefaction were observed in moraine and outwash deposits near Yakutat and elsewhere along the Yakutat Foreland by *Davis and Sanders* [1960]. The instability of these deposits along steep shorelines was dramatically demonstrated by the fact that in the 1958 event, three people who were on Khantaak Island near Yakutat (see Figure 2 for location), were killed by a large earthquake-triggered landslide and the local tsunami it generated [*Davis and Sanders*, 1960]. The landslide was located close to where Yakutat residents described disappearance of part of a native cemetery into the sea after the 1899 earthquake and where *Tarr and Martin* [1912, p. 79, Plate XIV] measured maximum shoreline subsidence of 2.1 m (7 feet).

In summary, 1905 and subsequent measurements of uplift or no change characterizes all shorelines consisting of bedrock as well as much of the shoreline in unconsolidated deposits (Figures 3, 4). In contrast, shorelines reported as submerged during the earthquakes are invariably in water saturated unconsolidated deposits that were particularly susceptible to surficial compaction, lateral spreading, and slumping due to the strong shaking, such as occurred during the 1899 earthquake sequence. Clearly, measurements of vertical shoreline changes in such deposits are not a reliable indication of tectonic subsidence or relative stability in coastal areas.

3.2. Shoreline displacement in the Yakataga area

In 1899 Yakataga was a small community of gold prospectors and trappers located just west of a reef (Yakataga reef) on the open ocean coast 160 km west of Yakutat (Figure 1). Residents noted that Yakataga reef and the beach at the boat landing just west of the reef were uplifted about 90 cm (3 feet) at the time of the September 4th earthquake (Figure 1). Although *Tarr and Martin* did not visit this locality, they obtained eyewitness accounts about the uplift there from questionnaires and newspaper articles that are cited in their publications [1906, 1912]. During the earthquake, the tide reportedly was at half ebb and receded to low water in twenty minutes (presumably due to the uplift). There was no tsunami reported at Yakataga or elsewhere along the Gulf of

Alaska coast, which suggests that vertical displacement was probably small and limited in its offshore areal extent.

Yakataga Reef is on the hanging wall of the Sullivan fault, a north-dipping thrust that trends west roughly parallel to the coast for about 40 km from west of Icy Bay to just east of Yakataga Reef where it turns sharply southward to extend offshore as shown in Figure 1 [Miller, 1960]. The reported 90 cm uplift of the reef and boat landing at Yakataga in 1899 would be compatible with coseismic slip on the Sullivan fault during the earthquake of September 4th. In this area, an uplifted beach about 120 ± 30 cm above extreme high storm tide is still visible. The beach supports a spruce forest. Tree ring counts of stumps of the largest trees at the seaward edge of the forest date to within a few years of 1899 and are compatible with the reported coseismic uplift. We infer that coseismic slip on the Sullivan fault is a likely cause of the uplift at Yakataga. However, we can not preclude the possibility that the Sullivan fault is inactive, and that the 1899 uplift at Yakataga resulted from slip on an unidentified fault offshore.

Marine terraces that extend 50 km east of Yakataga to Icy Bay were studied by U.S. Geological Survey regional field mapping parties in 1951 by D.J. Miller and colleagues and sporadically between 1974 and 1999 by one of us (G.P.). Three laterally continuous, west-sloping marine terraces have been mapped for 50 km between Yakataga and Icy Cape near the west shore of Icy Bay (Figure 1). Minimum ages of the terraces in the Icy Cape area were determined by conventional radiocarbon dating of peat samples collected from sediments exposed at or near the base of the marine sequences on the terraces. The available data suggest long time intervals (at least 1,150 years) between the three major uplift events, at least 8 to 16 meters of coseismic (and possible interseismic) uplift per event, and an average late Holocene uplift rate of about 10 mm/yr [Plafker *et al.*, 1982]. Smaller uplift events of a few meters or less occurred in 1899 along this coast at Yakataga [Tarr and Martin [1912], and possibly also at Icy Cape [Jacoby and Ulan, 1983]. However, uplift in 1899 does not compare in vertical displacement to the older terraces. Some of the uplift and westward tilting, however, may be enhanced by rapid isostatic rebound related to glacial unloading since about 1900 in the Icy Bay and Malaspina Glacier region to the east [Sauber *et al.*, 2000]. Based on the pre-1899 terrace data, it has been ~1300 years or more since the last major terrace-forming event at Icy Cape and, at a long-term average uplift rate of ~10 mm/yr, the next great earthquake could involve uplift on the order of 10 to 13 meters.

The structure along which the pre-1899 terraces in the Icy Bay area were uplifted is unknown. A likely possibility is that it may be a northeastward extension of the Pamplona zone of faults beneath Icy Bay to connect with the onshore Malaspina fault (Figure 1). The Pamplona and Malaspina faults are part of a complex regional southeast to east-verging late Cenozoic fold and thrust belt that essentially link the eastern Aleutian megathrust with the Fairweather transform fault as a trench-transform system. We speculate that the large terrace steps and prominent west-slope of the terrace sequence between Icy Bay and Yakataga record very large slip events during great tsunamigenic earthquakes.

3.3. Steep Fault Model of Tarr and Martin

Based on their study of the 1899 uplift, *Tarr and Martin* [1912] proposed that block movements on a system of concealed faults in the Yakutat Bay area caused the earthquakes of 10 September. They also concluded that the earthquake of September 4th and accompanying coseismic emergence of Yakataga Reef resulted from faulting further to the west—an interpretation with which we concur.

There are three major problems with the *Tarr and Martin* [1912] block fault model in the Yakutat Bay area. First, there was no surface evidence for vertical faults along the shores of Yakutat Bay at about a dozen localities where these inferred faults would have intersected the coast. Second, the positions of some inferred faults are controlled by places where there is a change from uplift, or no displacement, to subsidence. However, as noted previously, all shorelines along which subsidence was reported are areas of water saturated unconsolidated deposits where much, if not all, of the shoreline drowning is likely to have resulted from shaking-induced surficial compaction, liquefaction, and submarine slides on delta fronts, rather than to tectonic movements. Finally, the inferred fault system in the Yakutat Bay area, with a total length of less than 145 km is much too short to generate the great earthquake of September 10th. A compilation of worldwide data on surface fault length versus magnitude [*Bonilla et al.*, 1984; *Wells and Coppersmith*, 1994], indicates that earthquakes of M_w 8.1–8.2 magnitude would each have average rupture lengths of ~300 km. Clearly, the faults postulated by *Tarr and Martin* [1912] in the Yakutat Bay area sample only a fraction of the coseismic deformation that must have accompanied the great 1899 earthquake sequence.

3.4. Postulated Minor Faults

In addition to the inferred steeply dipping faults in the Yakutat Bay area, *Tarr and Martin* [1912] described zones of closely spaced fresh fissures and “V” shaped notches that roughly parallel topographic contours at several localities on the summits and flanks of steep ridges. They interpreted these features to be possible coseismic faults (short green bars, Figure 2). Those on The Nunatak are especially well-developed (Figures 5 and 6) and because they were reasonably accessible by boat, they were investigated in some detail. The fissures at The Nunatak were inferred to be steeply dipping faults with a left-oblique slip component. This interpretation is especially puzzling in light of the 1958 dextral strike-slip displacement on the Fairweather fault that extends beneath Nunatak Fiord along the northeast side of The Nunatak and is oriented almost parallel to the fissures described by *Tarr and Martin* [1912] (Figure 2). It should be noted, however, that the existence of the Fairweather fault was not discovered until long after the field studies by Tarr and Martin were completed, possibly because the segment of the fault trace along the northwest trending arm of Nunatak Fiord (and northwest of the fiord) was entirely beneath glacial ice and was virtually inaccessible by boat or foot (Figure 2).

One of us (G.P.) has re-visited most of these fissure swarms and reinterprets them as “sackung” formed by large-scale sudden gravitational slumping, rather than to fault slip. This interpretation is indicated by (1) their occurrence high on steep ridge slopes and ridge crests; (2) strike generally parallel to ridge contours or at a slight angle to them; (3) dip surfaces mainly into the slope that commonly results in prominent “V” shaped notches; (4) characteristic extensional surface openings; (5) local presence of ridge-parallel graben on or near the ridge summits; and (6) general non-coincidence with

geologic unit boundaries. Furthermore, the predominantly fresh appearance of the scarps in a region of active mass wasting and their common proximity to active faults suggests that they are formed or reactivated by strong earthquake shaking. For instance, the fissure swarm on The Nunatak is known to have been reactivated during the 1958 M7.9 Lituya Bay earthquake on the Fairweather fault [Tocher, 1960], the trace of which trends beneath Nunatak Fiord within about 1300 m of the zone of fissures (Figure 2). In fact, prominent fissure swarms and graben comparable to those on The Nunatak occur on the upper parts of steep-sided ridges along most of the 225 km-long onshore segment of the Fairweather fault as well as throughout much of the Yakutat Bay region.

The Nunatak fissure locality is at the north end of a northwest-trending linear ridge 9.4 km long, 500–1500 m wide, and as much as 475 m high along the southwest shore of Nunatak Fiord. West Nunatak Glacier covered all but the high northwestern end of the ridge at the time that the fissures were described by *Tarr and Martin* [1905]. Schistose and gneissic meta-sedimentary and meta-igneous rocks underlie The Nunatak except where concealed by recent glacial moraine deposits along the lower slopes. Bedrock foliation strike is N32–42°W and dip is 54–80°NE. The fissure swarm extends some 1100 m along the southwest side of the Nunatak between 456 m elevation at the ridge top to about 360 m elevation where bedrock is mantled by glacial moraine (Figures 5, 6). Most of the sub-parallel fissures dip steeply into the slope along the bedrock foliation with the downhill side relatively up and they cut obliquely down-slope towards the southeast. Widely-spaced joint sets trending generally north–south and east–west intersect, and locally offset, the fissures. It is the local southeasterly down-slope component of slumping of the ground surface between the fissures at this locality that may have given *Tarr and Martin* [1912] the mistaken impression that they were observing left oblique slip faulting (see inset, Figure 5). In 1909, Lawrence Martin revisited The Nunatak in an unsuccessful effort to try to find slickensides on the fissure surfaces that would support the oblique slip interpretation of their origin. He reported that none could be found and that it was probably because of weathering of the fissure surfaces since 1899 [*Martin*, 1910, p. 40].

4. A Revised Deformation Model

If one interprets reported submergence along shorelines composed of saturated unconsolidated deposits as a superficial effect of earthquake shaking, a significantly different model can be constructed by contouring the uplift data. This mainly involves a broad, linear upwarp averaging 2–3 meters over an area at least 50 km long by 30 km wide that is centered between the Yakutat fault at the southwestern edge of the mountains and the Boundary fault (Figures 2, 9a). The southwestern limit of the uplift is unconstrained beyond the shores of Russell Fiord.

Superimposed upon this broad upwarp is a smaller block-like area of marked uplift (Bancas block) that culminates in the record 14.4 m uplift about 3.2 km north of Bancas Point (Figure 2, 4). This extreme uplift is inferred to be controlled on the east and south sides by local faults of large displacement. The south side of the block is the Esker Creek fault along which an abrupt coseismic north-side-up displacement of ~10 m was observed at the west shore of Disenchantment Bay [*Tarr and Martin*, 1912]. The Esker Creek fault is inferred to be part of a fault system along the front of the foothills that

connects with the Yakutat fault to the east and the Malaspina fault near Icy Bay to the west (Figure 1). On the east side of the Bancas block, an offshore fault, the Bancas Point fault, is suggested by the pronounced linear north–south shoreline and the large change in uplift (~9 m) across Disenchantment Bay (Figure 2). The north side of the block is poorly constrained because of absence of offset shorelines at the head of Disenchantment Bay. The northern boundary we favor is the west-northwest trending Neogene Chaix Hills fault although the possibility that it terminates against the active Fairweather fault can not be ruled out (Figure 2). There are no known geologic or seismologic constraints to the eastern limit of 1899 displacement on the Bancas block

The 1899 uplift is located just south of the complex junction where the northwest-trending Boundary fault beneath Russell Fiord trends towards—and possibly into—the Chaix Hills fault near the north end of Disenchantment Bay. One possibility suggested by the position of the uplift relative to these major active faults is that the 1899 earthquake involved movement on the Boundary fault and the uplift represents bulging that is an end effect of strike-slip faulting at the northern end of the Boundary fault. A major difficulty with this interpretation is that it requires an unreasonably large slip on the Boundary fault to account for the uplift. The Boundary fault is a strand of the Fairweather fault that is not seismically active. However, 1899 displacement data along the shores of the northern arm of Russell Fiord suggest that it may have had as much as 2.2 m vertical coseismic offset for at least 8 km along strike with the northeast block relatively upthrown (Figures 2, 9a). The displacement appears to die out to the southeast of Russell Fiord because no 1899 shoreline offsets were observed in that segment of the coast and no surface ruptures were found along the mapped trace onshore where the fault is fairly well exposed [*Tarr and Martin, 1912; Tarr and Butler, 1909*].

The alternative possibility, that also requires a concealed fault, is to attribute the broad upwarp to reverse movement on a fault along the southern front of the mountains. In this model, the marked local uplift in the Bancas Point area would be attributed to slip mainly on the Esker Creek and Bancas Point faults. The absence of a recognizable trace could be explained if the 1899 slip was on surface faults that were either concealed beneath post-earthquake alluvial deposits, water, snow, and ice on land or they may be blind thrusts that did not rupture the surface.

The large number of sizable 1899 earthquakes, together with the location of the 04 September shock and its related uplift of the reef at Yakataga, suggest that the sequence involved displacement on one or more of the onshore late Cenozoic thrust faults for at least 160 km west of Yakutat Bay (Figure 1). The vertical movements apparently died out between Yakataga and the settlement of Katalla 120 km to the west, because no shoreline changes were noted by residents there. Yakataga is situated on the north flank of the Sullivan Anticline, a thrust faulted, actively-growing asymmetrical anticline, which trends east-west onshore and swings abruptly offshore towards the southwest at the reef [*Miller, 1957*]. The apparent absence of a tsunami during any of the major shocks is the best evidence available to indicate that the movement probably occurred mainly on one or more faults inland from the coast. The only other settlement along the mainland coast was a native village at Dry Bay, 90 km southeast of Yakutat (Figure 1). Although residents there reported on the intensity of shaking, no mention was made of either changes in shoreline elevation or unusual waves along the coast [*Tarr and Martin, 1912*].

5. Paleoseismology

On the northeast end of Krutoi Island (see Figure 2 for location) *Tarr and Martin* [1912, p.30, 42] noted an older narrow elevated terrace backed by an abandoned wave cut bluff at a locality where the beach was elevated 30 cm in 1899. The inner margin of the older terrace is 135 cm above the 1899 surface and is underlain by rudely stratified beach sand, gravel, and abundant shell fragments. When visited in 1979 (by G.P.), the surface had a growth of mature trees on it at least 130 years old based on tree ring counts for one core that did not reach the center of the tree. A shell sample (W-4489) from the surface of the older terrace yielded a ^{14}C date between 317 and 511 calendar ybp (380 ± 70 radiocarbon ybp). This date is considered to be a minimum age for emergence of the terrace and possibly also a minimum recurrence time for large 1899-type uplift events.

6. Earthquake Seismograms and Seismic Moment

A small number of damped long-period seismograms from Tokyo, Japan and Catania, Sicily are available for the two largest earthquakes of the 1899 sequence, permitting us to examine the character of the long-period shear waves and use surface waves to estimate seismic moment. Recordings from a station at Tokyo ($\Delta=50^\circ$) are reproduced in Figure 8. These seismograms show the familiar features of modern long-period recordings, with distinct S-waves and well-developed 20 to 50-sec surface-waves clearly visible.

As Figure 8 shows, there are notable differences in the S-wave seismograms recorded at Tokyo for the 04 and 10 September events. The 10 September S-wave shows at least three distinctive long-period pulses and a duration of about three minutes, while the principal S-wave ground motion at Tokyo from the 04 September earthquake is complete in about one minute. Since the S-waves from 04 and 10 September shocks travel almost identical paths from source to station, the complex character of the 10 September seismogram must be due predominantly to complexity in the faulting during this earthquake. As is shown below, the pattern of ground uplift that occurred on 10 September in the Yakutat Bay region independently suggests earthquake rupture on at least 3 separate fault planes (see Figure 9b).

The true ground motion at Tokyo and Catania may be determined from the published instrumental constants for the two seismographs. Those for Catania have been obtained from *Lawson* [1908, p. 101] in the report on the 1906 San Francisco earthquake, and the Tokyo seismograph constants are given in *Publications of Earthquake Investigations in Foreign Languages* [1901, p. 10]. The damping in these systems appears to be inadvertent and due to friction of the moving parts, but for these recordings was sufficient to produce good long-period seismograms. Amplitude spectral densities of 50-second surface waves were obtained by Fourier analysis, corrected for instrument response and for propagation path effects using tables given by *Ben-Menahem et al.* [1970], and converted to seismic moment for various assumed faulting geometries. Amplitudes at longer periods could not be used because the Tokyo and Catania seismographs actually de-magnify ground motions at periods > 100 sec.

Best estimates of moments obtained from seismograms for both earthquakes are listed in Table 1. As is discussed below, distribution of uplift determined from raised shorelines within Yakutat Bay constrain the faulting during the 10 September event to be on north and northeasterly dipping thrust faults. We use the geometry of these model faults to correct spectral amplitudes from the 10 September surface waves for radiation pattern effects. To test the effect of differences in fault geometry on the moment determination, the orientation of the slip vector was varied from pure dip-slip motion to equal amounts of thrust and right-lateral strike slip movement (slip direction = 90° to 45°) on faults striking E–W (270°) and NNW (330°). The results of this test are shown in Table 2, and it is clear that the moment of the 10 September event cannot be less than about 10^{21} N-m or greater than $\sim 6 \times 10^{21}$ N-m. The 04 September shock was assumed to be pure dip-slip on an east–west striking and 30° north-dipping fault. Again, slight changes in strike dip, and slip vector orientation produced variations in moment similar to those shown in Table 2 for the 10 September earthquake.

It is important to note that although uncertainties in faulting parameters and the absence of >100 sec. surface wave amplitudes result in significant uncertainties in moment estimates, the available data do establish reliable minimum values for seismic moment. For example, with unknown faulting parameters the minimum moment corresponds to assuming the recording station lies on the maximum of the surface-wave radiation pattern. No upper limit can be determined, since in principle at least, Tokyo and Catania could both be arbitrarily close to a null in the radiation pattern. Similarly, if the duration of faulting is significantly longer than 50-sec., the seismic moment estimated from these relatively short period waves is again a minimum value. On this basis, the moments of the 04 and 10 September events are estimated to be no less than 10^{21} N-m.

Table 1 gives the seismic moment and moment magnitude, M_w , as well as the surface-wave magnitudes determined by *Abe and Noguchi* [1983] for the two events. Shown for comparison in this table are equivalent parameters determined for the 1906 San Francisco earthquake determined by *Thatcher et al.* [1997]. Clearly, both in terms of M_w and seismic moment, the two largest Yakutat Bay earthquakes are considerably more potent than the 1906 shock, even though their 20-sec. magnitudes are quite comparable.

7. Crustal Deformation and Faulting Models

Faulting models constructed to satisfy uplift data within Yakutat Bay independently argue for a complex mechanism of strain release during the 10 September earthquake. The uplift data shown by *Tarr and Martin* [1912, plate XIV] with some corrections based on more recent field work in the summers of 1973 and 1980 (Figure 2 and Appendices A and B) have been contoured approximately and are shown in Figure 9a.

The uplift contours provide some useful general constraints on the mode of faulting in the vicinity of Yakutat Bay. The northwest–southeast trending contours crossing the peninsula between Yakutat Bay and Russell Fiord as well as those between northern Russell Fiord and the Fairweather fault argue for northwest-striking, northeasterly dipping thrust faults in Yakutat Bay and the northern third of Russell Fiord. These may correspond to buried parts of the inferred northeast-dipping Yakutat thrust

fault (and possibly the smaller Otmeloi fault) along the east side of Yakutat Bay and the Boundary fault beneath the north arm of Russell Fiord. The large (6–14 m) localized uplifts on the northwest shore of Disenchantment Bay suggest significant amounts of slippage on both the north-dipping Esker Creek fault and the inferred west-northwesterly dipping Bancas Point thrust fault.

With these constraints in mind, a fault model that acceptably approximates the observed deformation in Yakutat Bay was constructed (Figures 9b, 10). Its parameters are listed in Table 3 and the vertical movements it produces are shown in Figure 9b. Geographic coordinates of the model faults and comparison of observed and computed uplift values are included in the on-line supplement (Appendices C and D). About 10 to 20 meters of slip are required on the three larger thrust faults, and the total cumulative seismic moment of these slip events is 0.58×10^{21} N-m. Strike-slip motion is not precluded by the uplift data, and roughly equal amounts of dip-slip and right-lateral strike-slip motion would produce better agreement with the seismically estimated moment. However, the discrepancy may not be significant, because the uplift data do not constrain possible right-lateral strike-slip movements on the Fairweather fault and faults within Yakutat Bay, or thrusting farther west on the Malaspina and related east–west striking late Cenozoic faults of the foothills fold and thrust belt. A schematic block diagram showing the main fault sources used in modeling in the Yakutat Bay area is shown on Figure 10. The most significant result of the comparison between the seismic and geodetic estimates of fault movements within the Yakutat Bay area is that crustal deformation there can account for no more than about 1/3 of the 10 September earthquake seismic moment. Therefore, most of the 10 September slippage, and all of the 04 September earthquake slippage must be accommodated elsewhere.

The large seismic moment of the 04 September event and probable location west of Yakutat Bay (Figure 7), along with the observation of ~1 m uplift at Yakataga (Figure 1) suggest that this earthquake represents large slip along late Cenozoic thrust faults in the foothills belt west of Yakutat Bay. No other active faults within this region but outside Yakutat Bay appear extensive enough to account for the large seismic moment (1.5×10^{21} N-m) of this shock. Fault slip must have been substantial. Even distributing slippage uniformly over a fault plane 150 km long and 50 km wide and matching the seismic moment would require about 7 m of slip across this zone.

8. Earthquake Hazards and Seismic Gaps

Several previous studies have examined the long-term seismic potential of the Yakataga-Yakutat region. On the basis of a reconnaissance study of displaced shorelines along part of the Gulf of Alaska coast, *Plafker* [1966] noted that the portion of the continental margin east of the 1964 earthquake focal region was a prime candidate for a major earthquake. Subsequently, *Sykes* [1971] mapped the rupture zones of 20th century great earthquakes along the Alaskan portion of the Pacific Plate margin. He identified a 200–300 km long region between Yakutat Bay and the 1964 focal region as a seismic gap, a segment of the plate boundary that is the likely site of a future **great ($M > 7.8$)** earthquake (Figure 7). On the other hand, *Kelleher* [1970] used similar great earthquake mappings but concluded that the gap between the focal regions of the 1964 and 1958

earthquakes was too small to sustain a great earthquake and/or may have ruptured completely in the 1899 earthquake sequence. The 1979 M7.4 St. Elias earthquake filled only a small part of the region between the 1964 and 1958 rupture zones (Figure 7).

Although our re-assessment of the 1899 earthquakes sheds new light on the seismic potential of the Yakataga region, the total extent of 1899 rupture remains poorly resolved. Figure 11 shows 4 distinct regions within which 1899 earthquake slip could have occurred. Our results show that there was locally large seismic slip in the vicinity of Yakutat Bay (western end of region A) and that it probably extended west at least as far as Yakataga (regions B and C).

However, the 1899 slip must have been more widespread. Analysis of seismograms constrains the cumulative seismic moment of the two largest earthquakes to be $\sim 3 \times 10^{21}$ N-m, about a factor of 5 larger than the moment release due to slip within the Yakutat Bay area computed from the fault model that matches uplifted shoreline data within the bay (Figure 9b). Extension of the 1899 faulting west to Yakataga (segments B and C, Figure 11) is unlikely to have made up this deficit. Table 4 demonstrates this, listing the 4 segments shown in Figure 11 and providing estimates of M_w and M_0 based on their approximate fault areas using the empirical fault area-moment magnitude relation of *Wells and Coppersmith* [1994]. The expected cumulative moment due to slip on segments B and C is $\sim 0.5 \times 10^{21}$ N-m, and even considering the inevitable uncertainties inherent in empirical rules like the area-moment relation, the deficit remains significant.

We therefore consider it likely that the 1899 earthquakes also ruptured parts or even all of segments A and D but available evidence does not permit us to be more specific. One tidy scenario would posit that the 04 September event, which produced ~ 1 m uplift at Yakataga with its epicenter nearby, was caused by slip on segments D, C, and possibly B. Confining the 10 September earthquake to all of segment A would then account for the remainder of the cumulative moment release and match the seismically estimated moment of the event. However, given observational uncertainties in the seismically estimated moments and imprecision in the empirical fault area-moment relation, other more complex scenarios cannot be ruled out.

Not all the complex plate boundary deformation zone shown in Figure 11 was ruptured in 1899, and significant additional strain has accumulated along the entire zone since that time. In particular, the offshore portions of the Pamplona zone and the Transition fault did not slip in 1899. Our results thus reinforce previous geologic and seismic studies suggesting the area is the likely site for a future major earthquake. This possibility has important implications not only because of the potential hazard to this part of Alaska, but also because a major plate boundary earthquake might well be accompanied by a tsunami that could inundate coastal areas of southern Alaska, British Columbia, and the Pacific northwest.

9. Summary and Conclusions

Our reinterpretation of the tectonics of the 1899 earthquake sequence suggests the following:

1. The seismicity and deformation are centered along the southern foothills of the Chugach and Saint Elias Mountains (Figure 11). Surface deformation during the 04 September M_w 8.1 event probably extends west of Yakutat Bay at least 160 km, and possibly as much as 250 km; for the 10 September M_w 8.2 event it extends at least 25 km southeast from Yakutat Bay to Russell Fiord, and perhaps as much as 200 km.
2. Earthquake-related deformation was primarily uplift and onshore. Deformation in the Yakutat Bay area during the 10 September event was due to slip on faults in the complex system of northward-dipping thrust faults or dextral-oblique thrust faults that lie between the Gulf of Alaska coast and the Fairweather-Chugach-Saint Elias fault system (see simplified block diagram in Figure 10). About one meter of uplift occurred along the coast at Yakataga. The apparent absence of a tsunami along the outer coast during both events suggests that there was no significant vertical displacement offshore.
3. In the Yakutat Bay area, coseismic vertical displacements of shorelines define a northwest-trending broad regional upwarp as much as 4.6 meters high on which is superimposed a relatively small fault-bounded block that is uplifted as much as 14.4 m on the west side of Disenchantment Bay (Figure 9a). Areas of reported shoreline subsidence in unconsolidated deposits (Figure 2) probably resulted mainly from shaking-related surficial compaction, landspreading, and sliding rather than to tectonic displacements.
4. Waves that accompanied the earthquake near the head of Yakutat Bay were probably generated by a combination of tectonic uplift, submarine slides, and rock and ice avalanches into the bay. They did not cause inundation at Yakutat near the bay mouth.
5. Swarms of fissures and related graben on steep slopes and ridge tops (sackung) that were interpreted as subsidiary faults at The Nunatak and elsewhere [Tarr and Martin, 1912] are mainly caused by earthquake-triggered gravitational spreading and slumping, and are not fault scarps.
6. According to our reappraisal, the focal region of the 1899 earthquake sequence is not likely to have filled the offshore segment of the seismic gap that lies between the source regions of the 1964 Alaska and the 1899 earthquakes. If correct, this part of the plate boundary probably has a relatively high potential for a future major tsunamigenic earthquake along the complex fault boundary that extends from the eastern end of the Aleutian Megathrust ~250 km to the Fairweather transform fault in the vicinity of Yakutat Bay (Figure 1).

Acknowledgments. Careful reviews were provided by J. C. Savage and C. W. Wicks, Jr. Travis Hudson, Ron Bruhn, and Terry Pavlis assisted with re-measurement of heights of uplifted terraces in Yakutat Bay during 1979 and 2000; Ed Roth participated in leveling across the sackung on The Nunatak in 1967 (Figure 5). Luke Blair created a digitized data base from Tarr and Martin's published map showing coseismic displacements (Appendix A), and prepared figures 2 and 9. V.J. Labau of the U. S. Forest Service made available an extensive data base of tree ages from the post-1899 forest along the east side of Yakutat Bay.

References

- Abe, K., and S. Noguchi, 1983, Revision of magnitudes of larger shallow earthquakes, 1897–1912, *Phys. Earth Planet. Int.*, 33, 1–11.

- Ben Menahem, A. M. Rosenman, and D. G. Harkrider, 1970, Fast evaluation of source parameters from isolated surface wave signals, 1, Universal tables, *Bull. Seismol. Soc. Am.*, 60, 1337–1387.
- Bonilla, M.G., R.K., and J.J. Lienkeamper, 1984, Statistical relations among earthquake magnitude, surface rupture length, and surface fault displacement: *Bull. Seismol. Soc. of Am.*, 74, 6, 2379–2411.
- Bruhn, R.L., T.L. Pavlis, G. Plafker, and L. Serpa, 2004, Deformation during terrane accretion in the Saint Elias Orogen, Alaska: *Geol. Soc. Am. Bull.*, 116, 7–8, 771–787
- Davis, N. T., and N.K. Sanders, 1960, Alaska earthquake of July 10, 1958: Intensity distribution and field investigation of northern epicentral region: *In*, Tocher, Don, ed., The Alaska earthquake of July 10, 1958, *Bull. Seismol. Soc. of Am.*, 50, 2, 221–252.
- DeMets, C., R. G. Gordon, D. F. Argus, and S. Stein, 1990, Current plate motions, *Geophys. J. Int.*, 101, 425–478.
- Doser, D., 2006, Relocations of earthquakes (1899–1917) in south-central Alaska, *Pageoph.*, 163, 1461–1476.
- Elliott, J., J. T. Freymueller, C. F. Larsen, 2007, Untangling the tectonics of the St. Elias Orogen, Alaska, using GPS, *this volume*, submitted.
- Fletcher, H. J., J. T. Freymueller, 1999, New constraints on the motion of the Yakutat block, *Geophys. Res. Lett.*, 26, 3029–3032.
- Hudson, Travis, G. Plafker and M. Rubin, 1976, Uplift rates of marine-terrace sequences in the Gulf of Alaska, *U.S. Geol. Surv. Circ.* 733, 11–13.
- Jacoby, G.C. and L.D. Ulan, 1983, Tree ring indications of uplift at Icy Cape, Alaska, related to the 1899 earthquakes, *J. Geophys. Res.*, 88, B11, 9305–9313.
- Kelleher, J., 1970, Space-time seismicity of the Alaska-Aleutian seismic zone, *J. Geophys. Res.*, 77, 5745–5756.
- Lahr, J.C., G. Plafker, C.D. Stephens, K.A. Fogelman, and M.E. Blackford, 1979, Interim report on the Saint Elias earthquake of 18 February 1979: *U.S. Geological Survey Open File Report 79, 670, 35*
- Lawson, A. C., 1908, The California earthquake of April 18, 1906, *Report of the State earthquake Investigation Commission, Carnegie Institution of Washington, D.C.*, 2, 641.
- Martin, L., 1910, Alaskan earthquakes of 1899. *Geol. Soc. of Am. Bull.*, 21, 339-406.
- Miller, D.J., 1957, Geology of the southeastern part of the Robinson Mountains, Yakataga district, Alaska: *U.S. Geol. Surv. Map OM-187*.
- Miller, D.J., 1961, Geology of the Lituya district, Gulf of Alaska Tertiary province: *U.S. Geol. Surv. Map OM-187.etc*
- Pavlis, T.L., C. Picornell, L. Serpa, R.L. Bruhn, and G. Plafker, 2005, Tectonic processes during oblique-collision: Insights from the St. Elias orogen, northern North American Cordillera: *Tectonics*, 23, TC 3001, 1–14.
- Plafker, G., 1966, Holocene (Recent) vertical displacements in coastal south-central Alaska: A possible approach to prediction: *2nd U.S.-Japan Conference on Research Related to Earthquake Prediction, Lamont Geological Observatory of Columbia University, Palisades, New York, Proceedings*, 29–31.
- Plafker, G., 1969, Tectonics of the March 27, 1964 Alaska Earthquake, *U.S. Geol. Surv. Prof. Paper 543-I*, 74.
- Plafker, G., L.M. Gilpin, and J.C. Lahr, 1994a, Neotectonic map of Alaska, in G. Plafker, G. and H.C. Berg, eds., *Geol. Soc. Am., The Geology of North America, G1, Plate 12*.
- Plafker, G., T.L. Hudson, T. Bruns, and M. Rubin, 1978, Late Quaternary offsets along the Fairweather fault and crustal plate interactions in southern Alaska: *Can. Jour. of Earth Sci.*, 15, 5, 805–816.
- Plafker, G., T. L. Hudson, M. Rubin, and K.L. Dixon, 1982, Holocene marine terraces and uplift history in the Yakataga seismic gap near Icy Cape, Alaska, *in* W. L. Coonrad, ed., *U. S.*

- Geol. Surv. in Alaska, Accomplishments during 1980, U.S. Geol. Surv. Circ. 844*, 111–115.
- Plafker, G., J.C. Moore, and G.R. Winkler, 1994b, Geology of the southern Alaska margin, G. Plafker and H.C. Berg, eds., *Geol. Soc. Am., The Geology of North America, G1*, 389–449.
- Sauber, J., G. Plafker, B.F. Molnia, and M.A. Bryant, 2000, Crustal deformation associated with glacial fluctuations in the eastern Chugach Mountains, *J. Geophys. Res.*, *105*, 8055–8077.
- Sykes, L.R., 1971, Aftershock zones of great earthquakes, seismicity gaps, and earthquake prediction for Alaska and the Aleutians, *J. Geophys. Res.*, *76*, 8021–8041.
- Tarr, R.S., and B.S. Butler, 1909, The Yakutat Bay region, Alaska; Physiography and glacial geology, *U.S. Geol. Surv. Prof. Paper 64*, 183.
- Tarr, R.S., and L. Martin, 1906, Recent changes of level in the Yakutat Bay region, Alaska: *Geol. Soc. Am. Bull.*, *17*, 29–64.
- Tarr, R.S., and L. Martin, 1912, The earthquakes at Yakutat Bay, Alaska, with a preface by G. K. Gilbert, *U.S. Geol. Surv. Prof. Paper 69*, 135.
- Thatcher, W., G. Marshall, and M. Lisowski, 1997, Resolution of fault slip along the 470-km-long rupture of the great 1906 San Francisco earthquake and its implications, *J. Geophys. Res.*, *102*, 5353–5367.
- Tocher, D., 1960, The Alaska earthquake of July 10, 1958: Movement on the Fairweather fault and field investigation of southern epicentral region: *Bull. Seismol. Soc. Am.*, *50*, 2, 267–292.
- Wells, D.L. and K.J. Coppersmith, 1994, New empirical relationship among magnitude, rupture length, rupture area, and surface displacement: *Bull. Seismol. Soc. Am.*, *84*, 974–1002.

Table 1. Seismic moment (M_0) and magnitude determinations for 1899 Yakutat Bay, Alaska earthquakes. M_s is the 20-sec. surface-wave magnitude determined by *Abe and Noguchi* [1983], and M_w is the moment magnitude.

Event	M_s	M_w	M_0 (10^{21} N-m)
04 Sept. 1899	7.9	8.1	1.5
10 Sept. 1899, 17:04 GMT	7.4	-	-
10 Sept. 1899, 21:41 (Average)	8.0	8.2	1.8
10 Sept. 1899, Catania, Italy	8.0	8.2	1.8
10 Sept. 1899, Tokyo, Japan	8.0	8.2	1.8
18 April 1906, San Francisco	8.0	7.8	0.4

Table 2. Variation in seismic moment determinations for 10 September 1899 event due to changes in fault plane orientation and direction of slip (90° corresponds to pure thrust motion and 45° to equal dip slip and right-lateral strike slip).

Strike	Dip	Slip Direction	Moment (10^{21} N-m)		
			Love-Catania	Raleigh-Catania	Love-Tokyo
270°	30°	90°	4.7	0.5	1.1
		60°	4.6	0.8	7.2
		45°	31.0	0.5	1.9
330°	30°	90°	3.1	0.6	1.8
		60°	5.9	1.9	2.6
		45°	3.2	1.6	1.7

Table 3. Model parameters for fault segments used to synthesize vertical deformation in Yakutat Bay. Refer to Figure 9b for location of numbered faults.

Fault	Length (km)	Width (km)	Depth (km)	Slip (m)	Strike	Dip	Moment (10^{21} N-m)
1	50	15	5	10	150°	30°NE	0.23
2	20	5	1.7	10	150°	10°NE	0.03
3	35	15	1.3	20	20°, 90°	30°NW, 30°N	0.32

Table 4. Areas of the 4 fault segments shown in Figure 11, with seismic moment (M_0) and moment magnitude (M_w) predicted from the empirical moment-area relationships [*Wells and Coppersmith*, 1994].

Fault Segment	Area (km ²)	M _w	M ₀ (10 ²¹ N-m)
A (Yakutat Bay/Lituya)	5300	8.1	1.8
B (Malaspina)	3000	7.7	0.3
C (East Yakataga)	2000	7.5	0.2
D (West Yakataga)	4000	7.9	1.1
<i>Compare with:</i>			
Yakutat Bay Fault Model	1375	7.8	0.6
04 September Earthquake		8.1	1.5
10 September Earthquake		8.1	1.8

FIGURE CAPTIONS

Figure 1. Tectonic setting of the 1899 Yakutat Bay earthquakes (red stars) showing inferred coseismic faults (red), Yakutat terrane (yellow), and major late Cenozoic onshore and offshore faults [Plafker *et al.*, 1994 a, b]. Fault name abbreviations: BF- Boundary fault; CHF- Chaix Hills fault; CSFS- Chugach-Saint Elias fault system; DRZ- Dangerous River fault zone; FF- Fairweather fault; KIZ- Kayak Island fault zone; MF- Malaspina fault; PZ- Pamplona fault zone; RMF- Ragged Mtn fault; SF- Sullivan fault; TFS- Transition fault system; WF- Wingham fault; YF- Yakutat fault. Inset shows revised interpretation of coseismic thrust faulting in the Yakutat area based on this study and reinterpretation of data in *Tarr and Martin* [1912].

Figure 2. Sites where vertical displacements of shorelines were measured by *Tarr and Martin* [1912] (Appendix A), and during this study. Red crosses denote uplift, green triangles subsidence; new or revisited sites of uplift measurements indicated by black crosses (Appendix B). Numbers next to symbols give uplift in meters at selected sites. Vertical faults (dashed black lines) and minor faults (short green bars) were inferred by *Tarr and Martin* [1912]. Thrust faults inferred in this study are shown by solid black lines with teeth on the upthrown blocks. The strike-slip Fairweather fault is shown for reference; it was not known at the time of the study by *Tarr and Martin*.

Figure 3. Air view (1980) to the south showing the 1899 marine terrace along the east shore of Yakutat Bay at Logan Beach that was formed by ~4.4 meters of coseismic uplift in 1899 (See Figure 2 for location). In this area, the inner margin of the terrace (dashed white line) is clearly marked by a change from a uniform age post-1899 forest on the terrace to older and higher trees inland as well as by local uplifted sea cliffs, beach ridges, or driftwood within the forest.

Figure 4. Air view [1980] to the north showing the elevated surf-cut terrace and sea cliff north of Bancas Point along the west side of Disenchantment Bay (See Figure 2 for location) where the maximum measured coseismic uplift of 14.4 m was measured by *Tarr and Martin* [1912].

Figure 5. Profile across zone of gravitationally-induced fissures (sackung) on the southwest flank of The Nunatak (see Figures 2 and 6 for location). Scarp height (V) and horizontal extension (H) in cm are indicated for the higher scarps. These features were interpreted by *Tarr and Martin* [1912, p.40] as evidence for minor left-oblique faulting during the 1899 earthquake as shown in the inset. See text for discussion.

Figure 6. Northwest air view (1967) near the north end of The Nunatak showing location of the middle and upper part of the profile in Figure 5, part of the swarm of northwest-trending fissures (sackung), and a major graben-bounding scarp 2.4 m high near the ridge crest at the right side of the profile (arrows). Many of these fissures were reactivated during the 1958 M7.9 Lituya earthquake.

Figure 7. Rupture zones of major 20th century earthquakes (shaded areas) around the northern Gulf of Alaska showing date and magnitude for each event. Locations of 04 and 10 September 1899 events obtained by *Doser* [2006] are shown for reference.

Figure 8. E–W seismograms of 04 and 10 September 1899 Yakutat earthquakes recorded at Tokyo ($\Delta=50^\circ$). Arrivals times of P, S, and ScS waves are shown for reference. Note single S-wave pulse of 04 September event and the several distinct pulses visible for the 10 September earthquake.

Figure 9. Observed (a) and computed (b) uplift. Contour interval is 150 cm except in vicinity of the Esker Creek-Bancas Point faults where uplift gradients are high and contour interval is 300 cm. Model faults are shown as dashed polygons in (b), with numbers in northeast corner keyed to listing of fault parameters (length, width, depth, dip, slip) given in Table 3.

Figure 10. Schematic block diagram showing principal thrust faults of the Yakutat Bay area (teeth on overthrust blocks) and horizontal projections of inferred slip planes for the 1899 earthquakes.

Figure 11. Cartoon showing possible primary slip area for the 1899 earthquake sequence (A–D). This scenario limits major slip to onshore or near-shore faults because the earthquakes did not generate a perceptible tsunami in the Gulf of Alaska. East of Yakutat Bay, the northern limit of slip is arbitrarily terminated at the Fairweather fault; west of the bay, it is terminated on the north by the Chugach-Saint Elias fault system and on the west by the approximate limit of surface deformation and aftershocks associated with the 1964 Alaska earthquake. See Figure 1 for explanation of fault symbols, and fault name abbreviations.

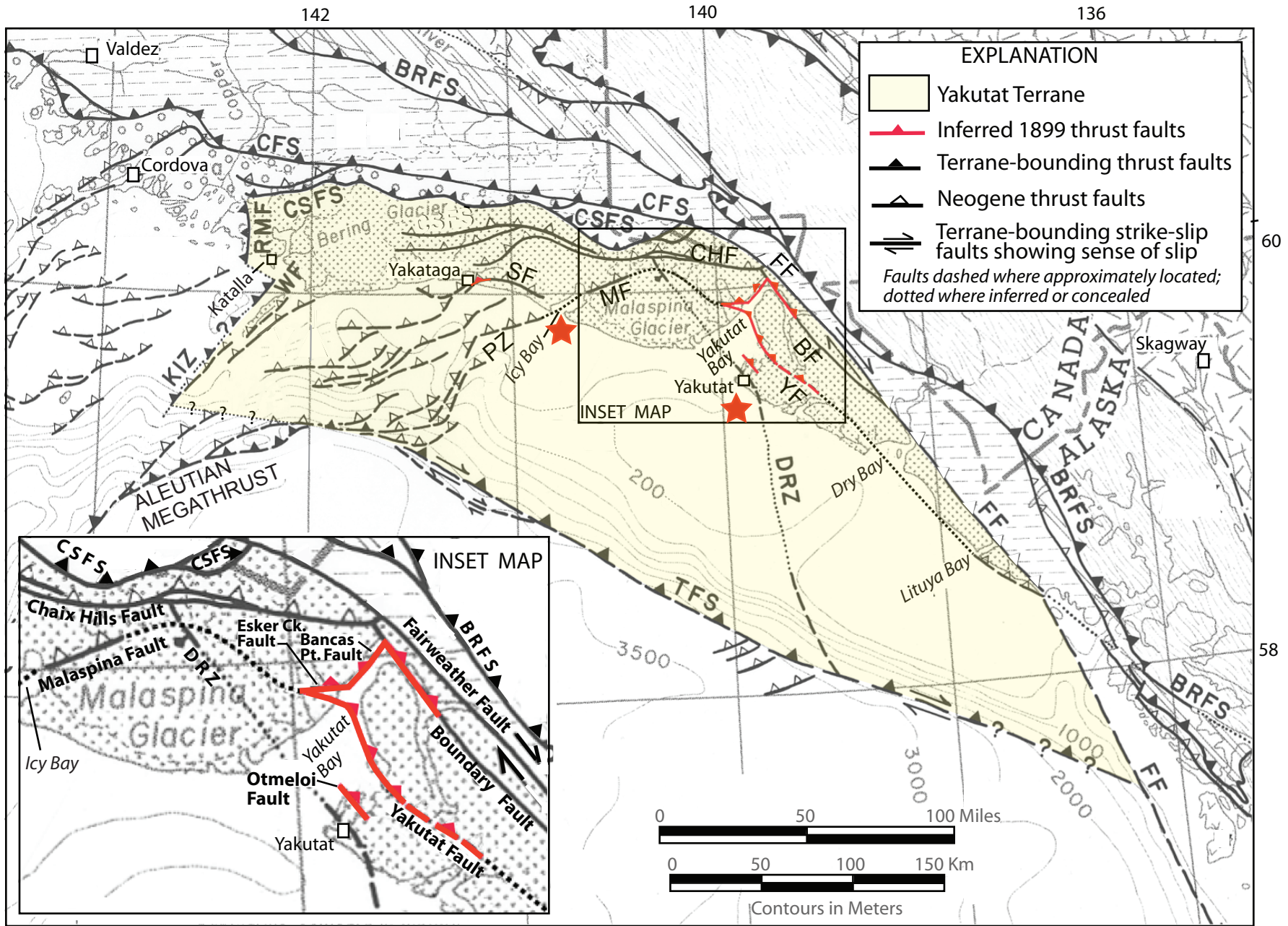


Figure 1.



Figure 3.

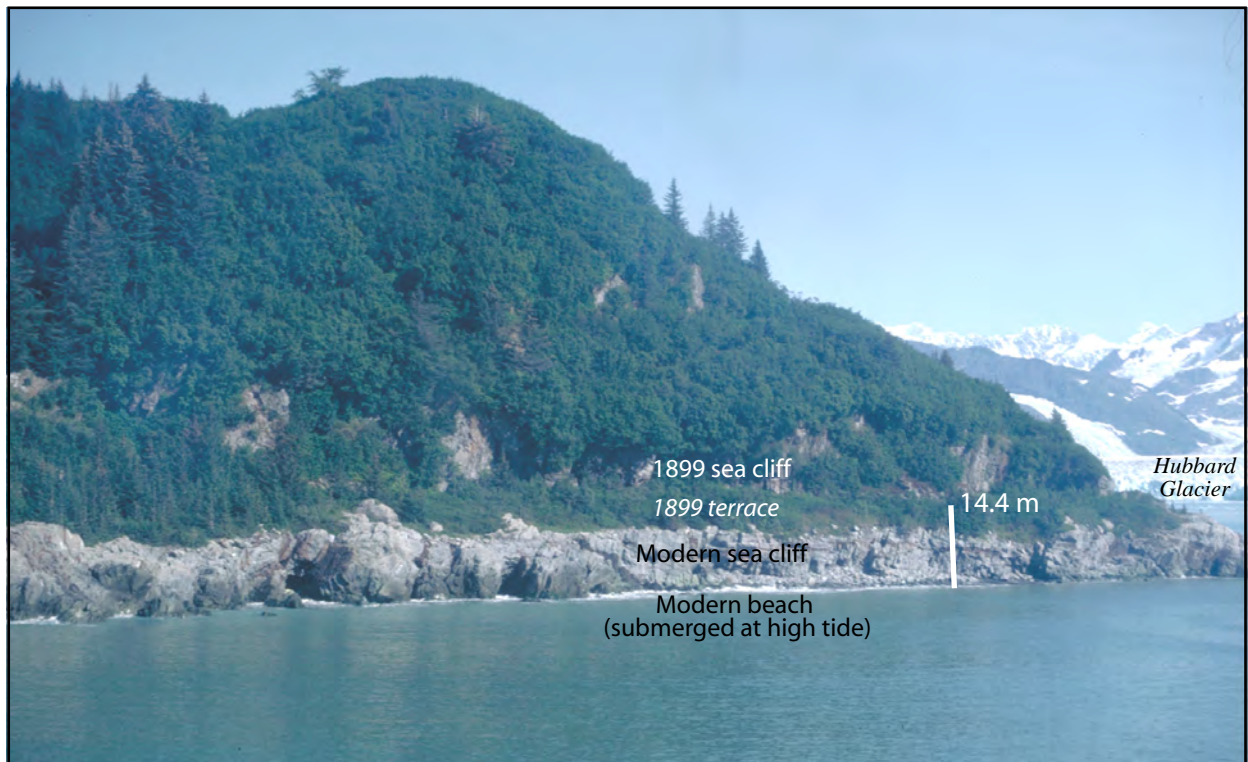


Figure 4.

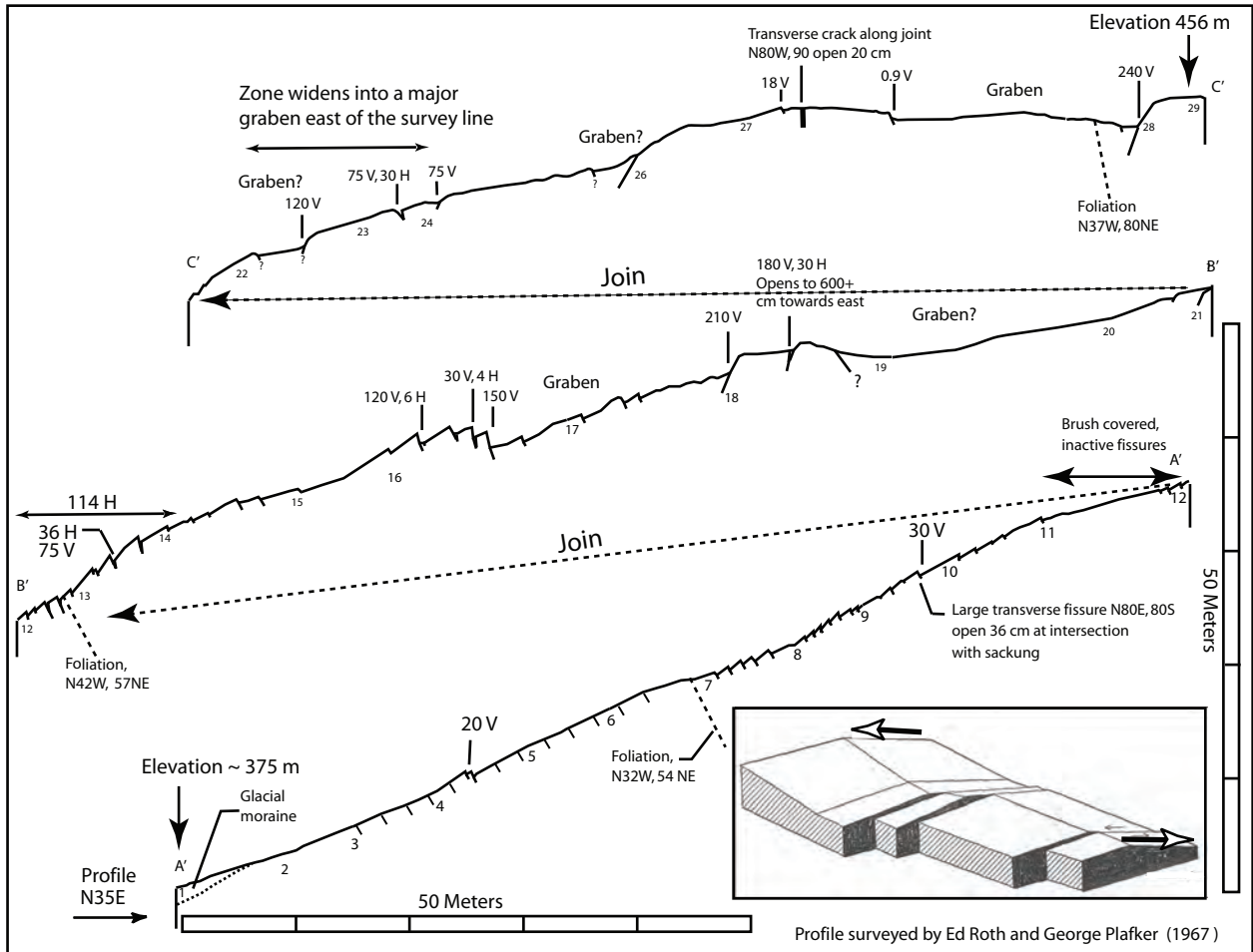


Figure 5.



Figure 6.

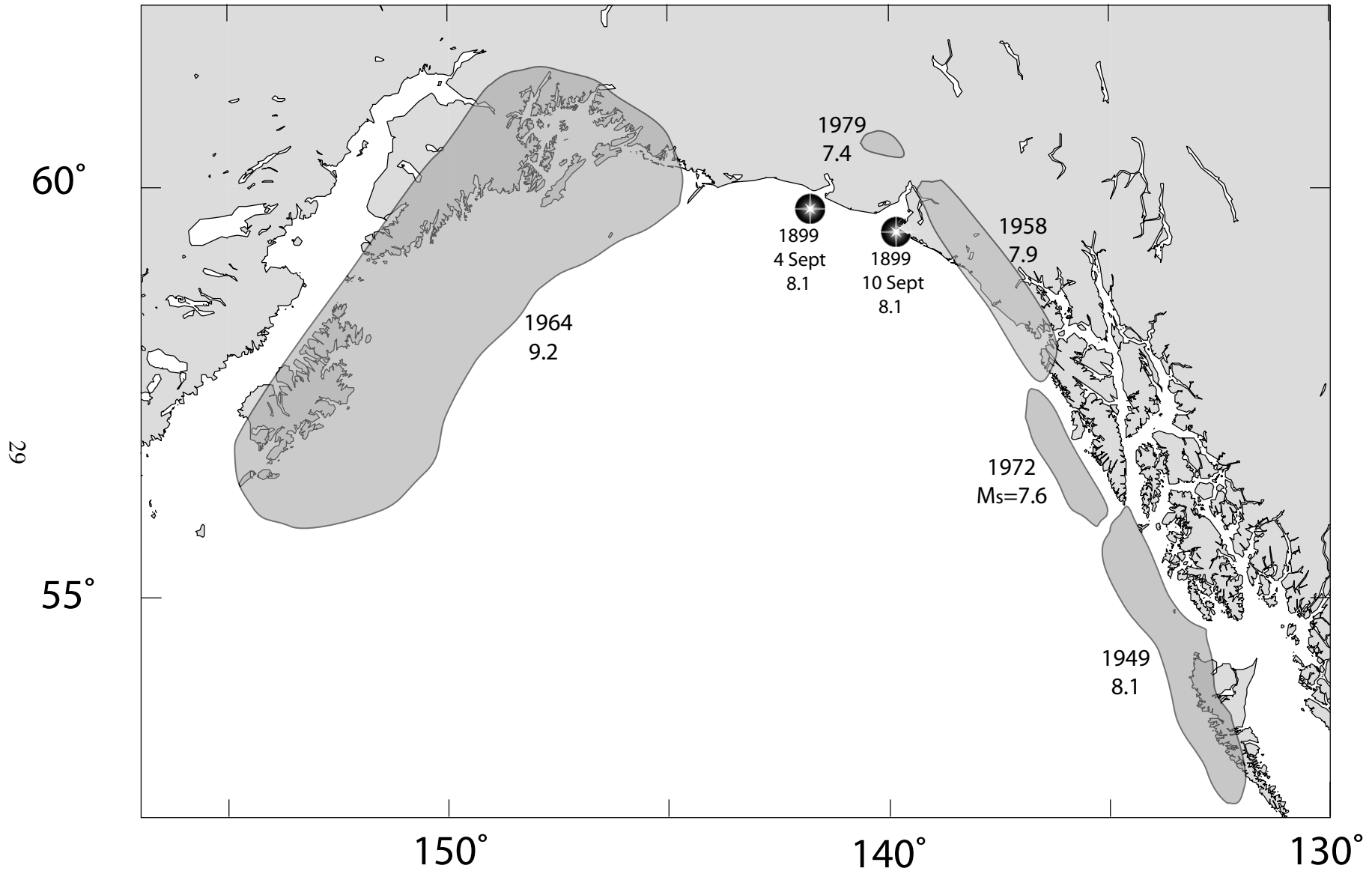


Figure 7

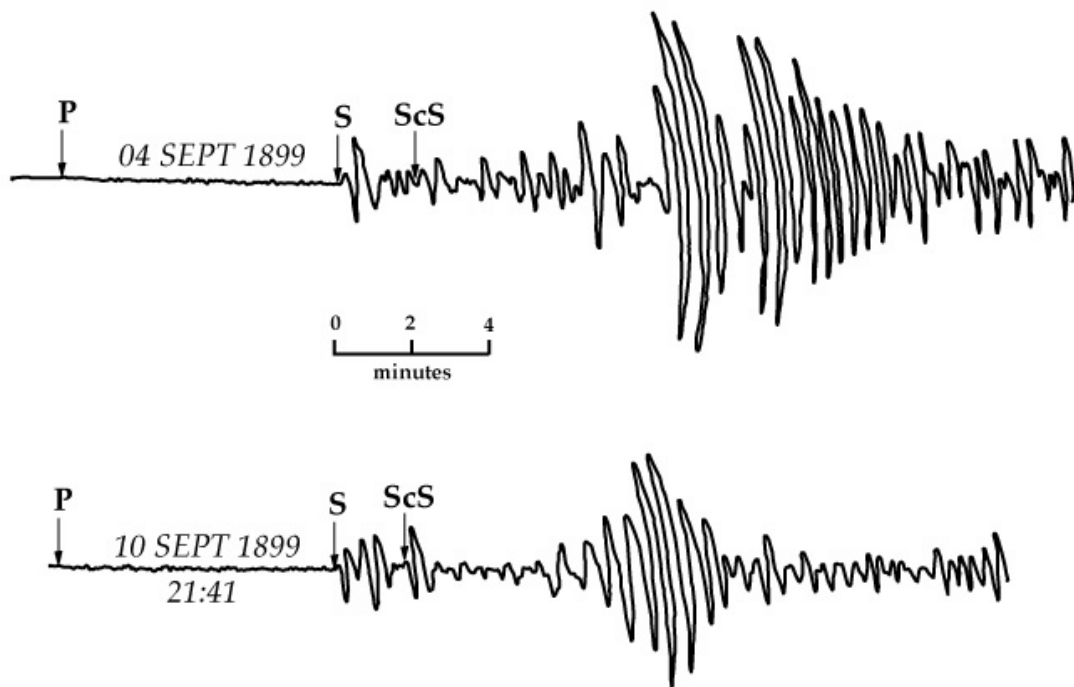


Figure 8.

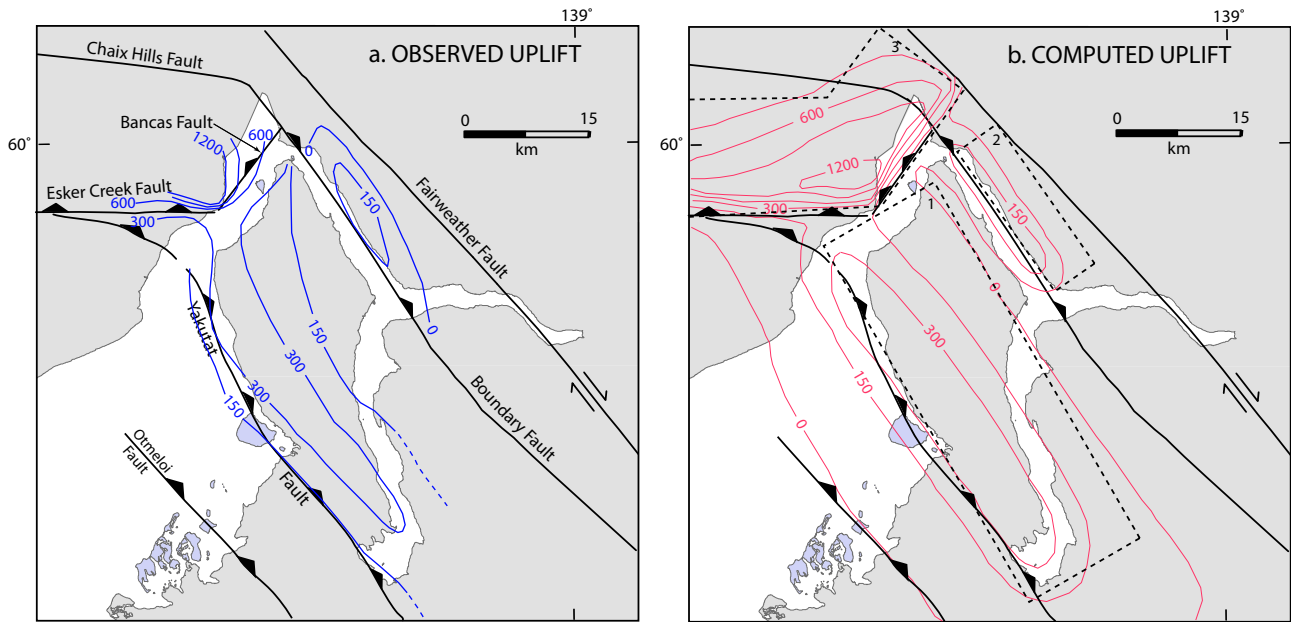


Figure 9:

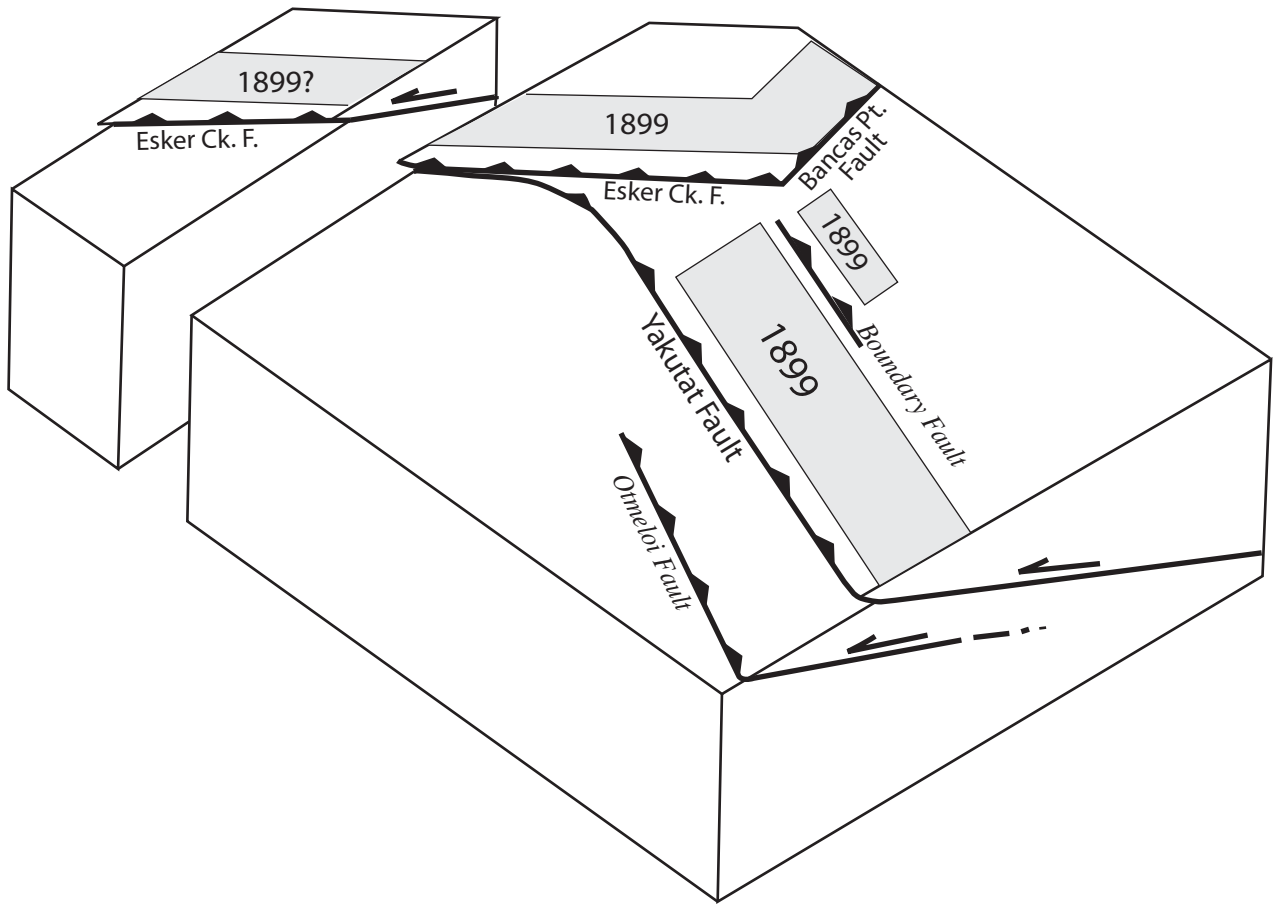


Figure 10

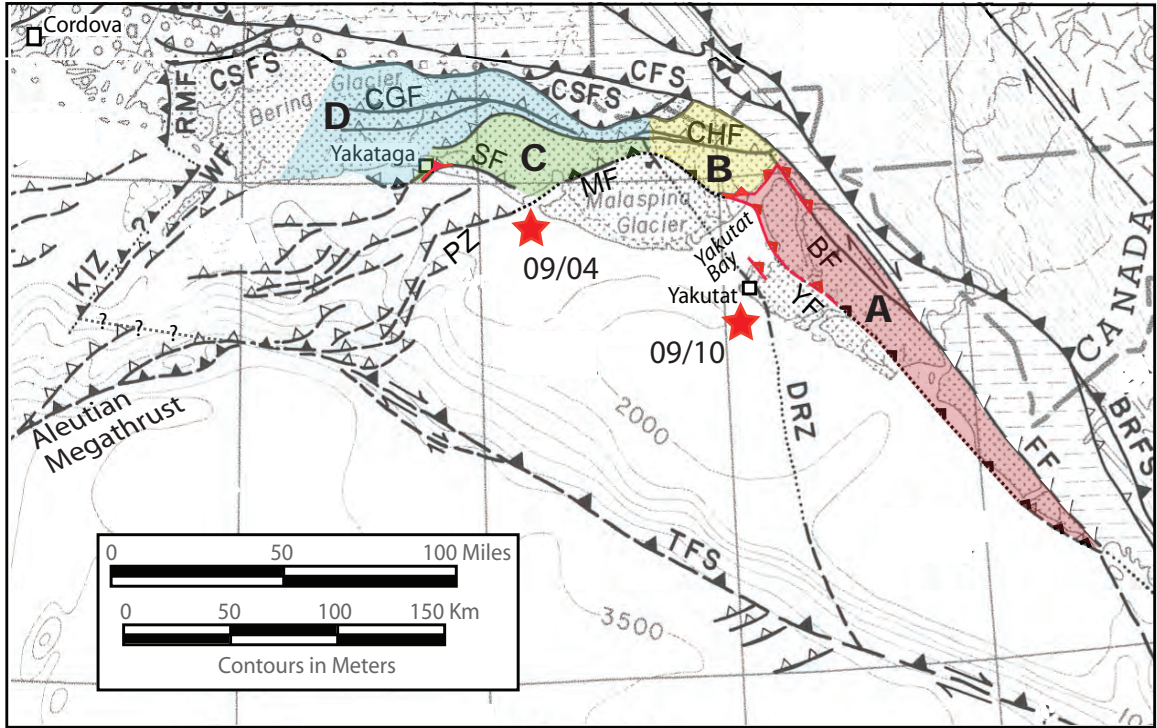


Figure 11.